A Model for Analyzing the Effects of Hydrodynamic Forces on Cell Adhesion in a Perfused Bioreactor

by

Bryan D. Owens

Submitted to the Department of Mechanical Engineering in Partial Fulfillment of the Requirements for the Degree of

Bachelor of Science
at the
Massachusetts Institute of Technology
June 2007

Signature of Author.....
Department of Mechanical Engineering
May 11, 2007

Certified by.....
Linda G. Griffith
SEHTI Professor of Biological and Mechanical Engineering
Thesis Supervisor

Accepted by.....
John H. Lienhard V
Professor of Mechanical Engineering
Chairman, Undergraduate Thesis Committee

A Model for Analyzing the Effects of Hydrodynamic Forces on Cell Adhesion in a Perfused Bioreactor

by

Bryan D. Owens

Submitted to the Department of Mechanical Engineering on May 11, 2007 in partial fulfillment of the requirements for the Degree of Bachelor of Science in Engineering as recommended by the Department of Mechanical Engineering

Abstract

In bioreactor culture systems that aim to provide a convective flux to address mass transport limitations of oxygen and other nutrients, large hydrodynamic forces and shear stress can potentially serve as a negative signals in tissue formation and morphogenesis. Shear stress and hydrodynamic forces may inhibit the formation of tissue from single cells by disrupting the integrin-mediated bonds with the extracellular matrix or the cadherin-mediated bonds with neighboring cells. In order to explore the relationship between the imposed forces and stresses from fluid flow and the inherent biological forces involved in cell adhesion, this thesis presents a simple model of cells in a planar array subject to perfused flow.

The modeling and sensitivity analysis of the system are covered within this thesis. Two models were built using first principles, and a range of physiological parameter values were used to estimate the forces and stresses generated by the perfusion flow. A third dynamical model from the literature was also employed. A computational approach using finite element modeling was also employed as a further tool for analysis. The resulting analyses yield valuable models that can model a range of cellular arrangements expected in a perfused bioreactor arrangement as a means to magnify and highlight the behavior at the microscale.

Thesis Supervisor: Linda G. Griffith
Title: S.E.T.I. Professor of Biological and Mechanical Engineering

This page has intentionally been left blank.

Acknowledgments

I would like to thank those individuals who made this thesis project possible. I would like to first thank Professor Linda Griffith. Serving the role of research mentor over the past three years, Professor Griffith has afforded me the opportunity to unify the fields of mechanical engineering and molecular and cellular biology in order to immerse myself in interesting research and begin to acquire the skills required of those in the research profession.

I would also like to thank the other members of the Griffith Lab. In particular, I would like to thank Walker Inman, Karel Domansky, Nate Tedford, Ta-Chun Hang and Matthew Lim. These individuals have spent countless hours with me since my first day in the lab teaching me the skills required by this field of research. They have helped me set up experiments, build models, and analyze large amounts of data. As I've learned, "It takes a village to raise a thesis," and the entire lab has had a positive influence on the writing of this thesis.

I would also like to thank those friends who particularly made my journey at MIT a complete one. I would like to thank the Godzillas: Brian, Carl, Christi, Diana, Elyse, Evelyn, and Yonas. I would also like to thank my fraternity, ZBT, for the countless hours of support particularly those from David, Jim, Mike, Rob, and Robert. I would also like to thank the friends who belong to neither of the prior groups: Anuja, Chris, Christa, Eitan, Hanhan, Jackie, Joy, Matt, Megan, Mitra, Nima, Rose, and Tulasi. You've all been with me through the ups and downs of my undergraduate career, and without your camraderie, MIT would have been a much different place.

Finally, I would like to thank my family. I first have to thank my mom. When I got into MIT, she said "You're going to MIT. You'll make it." I hope that this thesis demonstrates that while I have made it through this chapter of my life, I still have a large journey in front of me. I would also like to thank my siblings, Marlon, Kevin, and Daron for making me want to work even harder so that I could serve as a positive role model for their future. I would like to thank my grandparents, Ana and Pablo, who have counseled and supported me my entire life. I would like to thank my cousin, Alia, for being the one on the other end of the phoneline when the going got tough, and I contemplated my academic future.

Thank you to all those mentioned and not mentioned. My MIT voyage has been an amazing adventure. Onward and upward.

This page has intentionally been left blank.

Contents

List of Figures

List of Tables

Chapter 1

Introduction

Liver Tissue Engineering

The motivating application that has generated the central questions in this thesis is liver tissue engineering. In this form of tissue engineering, however, the end result is not replacement organ tissue, but rather microscale engineered tissue and organ constructs that can be used to investigate pathophysiology *in vitro*. In order to engineer such constructs, a high throughput microfluidic device has been developed as a robust platform for tissue engineering. This chapter will highlight the engineering as well as molecular and cellular biology necessary in order to motivate and frame the questions central to this thesis.

Three Dimensional Tissue Culture

Three dimensional cell culture systems have been demonstrated to provide a distinct advantage over conventional two dimensional culture systems in better recapitulating function and structure [4]. Cells are mechanically linked to their external environment. These physical links play im-

portant roles in communicating the physical microenvironment to the cell as well as modulating the response of the cell to a variety of other stimuli. Cells have been shown to transmit matrix forces in different ways depending on whether the cells are cultured in a two-dimensional versus three-dimensional environment [5]. The cellular response is a result of a family of factors including stress-strain transmission and adhesion. Culturing cells in a three-dimensional environment provides another dimension for external mechanical inputs and for cell adhesion. These interactions have direct effects on integrin and cadherin ligation, cell contraction, and the associated intracellular signals [6]. The three-dimensional microenvironment affects the diffusion of nutrients and growth factors which are crucial factors for the survival and formation of tissue and organ constructs. Furthermore, three-dimensional culture may be necessary to form certain complex structures such as the canilicular compartments of liver.

In order to understand how to appropriately engineer three dimensional tissue constructs, it is necessary to understand the mass transport of oxygen and other nutrients. By developing an understanding of the diffusion of media across a bulk tissue mass, it will motivate an understanding as to why perfusion culture is necessary for such applications. An instructive example appears below and is modeled in Figure 1.1.

Beginning from the continuity equation:

$$\frac{\partial C}{\partial t} = -\nabla \cdot \vec{N} + R, \tag{1.1}$$

where R is the reaction (in this case the oxygen consumption rate), $\vec{N}$ is the flux of oxygen, and C is the oxygen concentration.

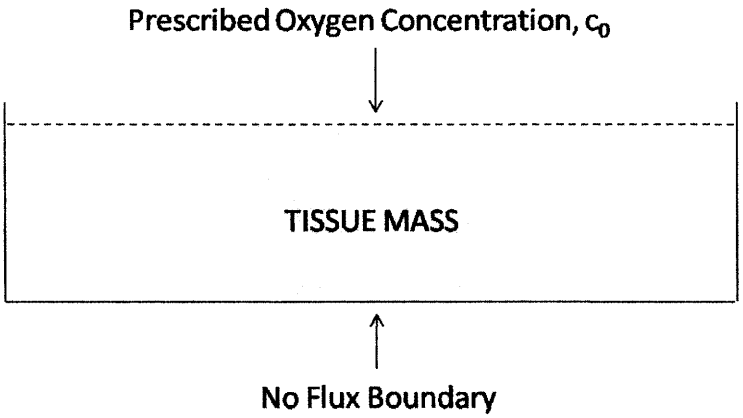

Figure 1.1: Instructive Example

Assuming steady state, the equation becomes:

$$\nabla \vec{N} = R \tag{1.2}$$

If flux is only generated from concentration gradients via diffusion, we can use Fick's Law shown by Equation 1.3.

$$\vec{N} = -D\nabla C \tag{1.3}$$

Combining Fick's Law with the continuity equation, the differential equation becomes:

$$D\nabla^2 C = R \tag{1.4}$$

If we assume one-dimensional diffusion, and that the oxygen concentration is known at the tissue

media interface and we also assume that there is no flux across the impermeable boundary, and then non-dimensionalize the resulting equation, we obtain the following equation.

$$\overline{C} = 1 - \frac{RL^2}{2DC_0}(2\overline{x} - \overline{x}^2), \tag{1.5}$$

where $\overline{C}$ is the non-dimensional concentration, $\overline{x}$ is the non-dimensional length, and D is the oxygen diffusion coefficient.

Recognizing the presence of the Thiele Modulus (ϕ) which is the ratio of the reaction rate over the diffusion rate, the equation then becomes:

$$\overline{C} = 1 - \frac{\phi^2}{2}(2\overline{x} - \overline{x}^2), \tag{1.6}$$

$$\text{where } \phi^2 = \tfrac{RL^2}{DC_0}.$$

Using reported literature values for the liver in this model, the thickness of a stimulated liver tissue construct that could be supported is approximately 110 μm. For a construct with an oxygen consumption rate typical of the pericentral region, the maximum thickness possible is near 190 μm.

Perfusion Tissue Culture

Recognizing that for the purpose of this application that larger constructs are necessary, the only way to accomplish this feat would be to increase the oxygen flux. The approach utilized here is to introduce a convective flux in order to increase oxygen transport.

Returning to 1.2 and instead using a modified expression for the flux:

$$N = -D\nabla C + vC,$$

where v is the bulk velocity of the media.

The differential equation for the oxygen concentration profile now becomes:

$$R = -v\nabla C + D\nabla^2 C \tag{1.7}$$

In this mass transport model, there is now a variable, v, that can be adjusted in order to influence the amount of oxygen seen by the cells at any time. The introduction of a perfused velocity now allows for tissue constructs of various sizes to be supported. A system that can harness the fact that the velocity can be adjusted in order to affect the local oxygen concentration will be a useful tool in order to successfully accomplish the goals set forth by three-dimensional hepatic tissue engineering.

Multiwell Bioreactor

Expanding upon a prior bioreactor design, a new high-throughput bioreactor has been developed [7]. The multiwell bioreactor is shown in Figure 1.2.

The plate has 12 identical units that contain reservoir and reactor wells. The reservoir well is filled with media, while the reactor well contains the tissue engineering scaffold in which the cells are seeded. Integrated pneumatic micropumps and capacitors enable bi-directional flow both up and down through the scaffold. By changing the frequency by which the micropumps open and close, different volumetric flow rates can be observed. In the reactor well, a sandwich assembly exists that consists of a gasket, a filter support, a microporous filter, a tissue engineering scaffold, and a

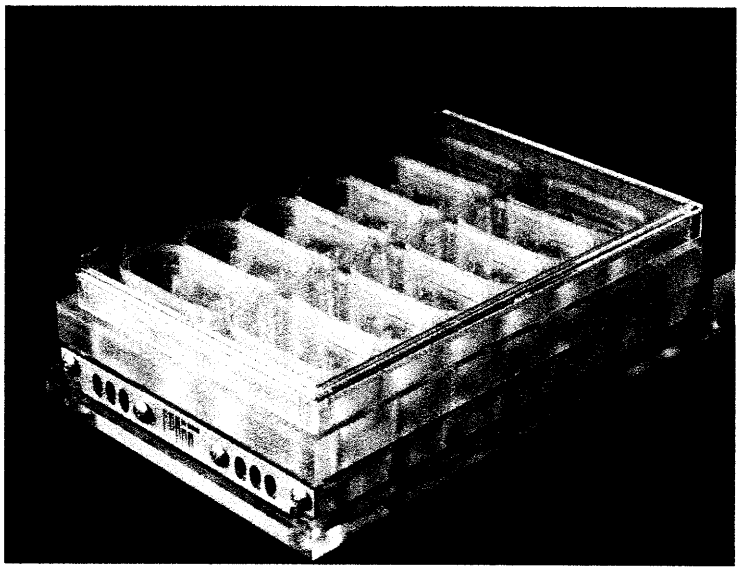

Figure 1.2: Multiwell Bioreactor

retaining ring. A schematic is shown in Figure 1.3.

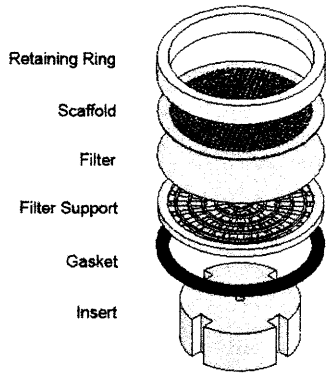

Figure 1.3: Reactor Well Components

The microporous filter serves as a resistive element to distribute the flow across the entire area of the scaffold. The scaffold itself has a concentric pattern of channels. Different types of scaffolds exist with varying numbers of channels. Each channel is approximately 300 μm x 300 μm. In order for the scaffold to be cell adhesive, the scaffold is soaked in a 30μg/mL solution of Type I collagen and phosphate buffered saline (PBS). After approximately 30 minutes, the exposed surfaces of the scaffold become cell adhesive.

Hepatocytes

For the purpose of liver tissue engineering, one of the main types of cells present in the liver is the hepatocyte. Estimates suggest that roughly 80% of the liver mass is a result of the contribution of the hepatocytes. Hepatocytes are responsible for a variety of the functions of the liver including protein synthesis, metabolism, and lipid export.

Hepatocytes are polygonal in shape, oftenly considered to be cuboidal in shape. Their faces are in contact with the sinusoids and other hepatocytes. On some of the lateral faces of the hepatocytes, modifications occur in order to form bile canaliculi. The cells have a radius of 10 μm.

Cell Adhesion Proteins

In order to form the complex assemblies required in the transition in levels of organization from cell to tissue, cells employ their molecular arsenal by means of a battery of adhesive molecules. Collectively, these molecules are referred to as cell adhesion molecules (CAMs). CAMs are spe-

cialized integral membrane proteins. These molecules mediate both cell-cell interactions as well as cell-matrix interactions. Within the large set of CAMs exist four major families. They include cadherins, immunoglobulin superfamily, integrins, and selectins. Figure 1.4 below shows the four major types of CAMs and their structure.

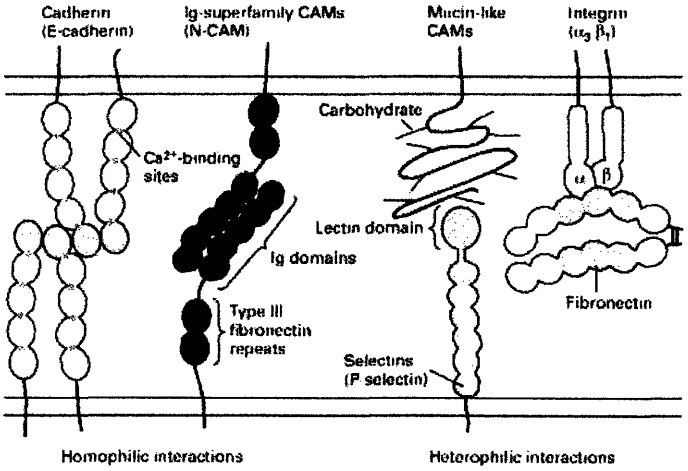

Figure 1.4: The four major types of cell adhesion molecules are here depicted [1].

The general structure of CAMs consists of multiple distinct domains. Some of these domains confer the ligand binding specificity. Adhesive interactions with other cells and extracellular matrix are mediated through the extracellular domains of CAMs. The portion of the CAMs that face the cytosol interact with adapter proteins that act as direct or indirect links to cytoskeleton components. Additionally, the adaptor proteins can be involved with intracellular signaling pathways. Intracellular molecules have also been shown to influence the intermolecular interactions of CAMs promoting their *cis* conformation and in turn causing local CAM clustering. Factors influencing nature of adhesion include binding affinities, binding kinetics, spatial distribution of CAMs, and external forces.

The two families of cell adhesion molecules of interest in this study are integrins and cadherins. These two varieties of cell-adhesion molecules are intimately involved in tissue engineering.

Integrins

Integrins consist of two distinct chains, an alpha (α) and a beta (β) chain. Multiple varieties of these chains exist, and the permutations of combinations of chains are responsible for the variety of extracellular matrix ligands bound by integrins. Bonds between the integrins and the extracellular matrix serve as anchors to prevent the cells from being removed from their environment[8]. The primary integrins present in hepatocytes are $\alpha_1\beta_1$ and $\alpha_5\beta_1$. In the multiwell bioreactor to encourage the formation of viable tissue constructs, we can manipulate the microenvironment by increasing the presence of extracellular matrix proteins such as collagen and fibronectin. The integrins are responsible for binding extracellular matrix and transducing the signals from the extracellular matrix to the cell [9].

In the context of this study, it is important to understand the mechanical properties of these bonds. Studies have been performed to measure the bond strength of integrins with techniques including atomic force microscopy, optical trapping, and magnetocytometry. The forces have been reported to be on the order of picoNewtons (10^{-12} N) [10, 11]. The picoNewton scale of these forces impose a required level of accuracy and detail in this model.

Cadherins

Cadherins are also mediators of adhesive interactions in the multiwell bioreactor. Cadherins are calcium dependent molecules that mediate tight binding between epithelial cells in tissue. Cadherins have intercellular, transmembrane, and extracellular domains. A proposed framework for the formation of cell-cell adhesion involves the following steps. The cadherins on one cell associate with other cadherins via their extracellular or cytosolic domains or both to form homodimers or higher order oligomers. These oligomers then interact with same or different CAM oligomers on adjacent cells. Cadherins can also be subdivided into different families, but the only distinction of importance here are the different classes of cadherins as they are relevant to adhesion studies. Cadherins with only one class will only bind to themselves; for example, E-cadherins, cadherins associated with epithelial cells, will only bind other E-cadherins via homophilic binding.

By similar techniques to those used in quantifying the strength of integrin-mediated bonds, the strength of cadherin-mediated bonds has also been quantified. Again, these forces or on the order of picoNewtons [12, 13].

Cell Seeding

When the cells are added to the system, they are suspended in solution and pipetted directly above the scaffold. Flow begins in the downward direction to pull the cells down into the scaffold channels. Once in the channels, the hepatocytes can adhere to the collagen coated scaffolds via integrin mediated binding or to one another via cadherin-mediated binding.

The cells are exposed to downward flow for a short period of time, approximately eight hours, in order to allow for the formation of focal adhesion complexes and other adhesive complexes. The flow is then reversed in order to remove dead cells and other debris that would interfere with tissue formation in the scaffold channels.

Conclusion

The subsequent chapters will utilize the presented background and engineering analysis in order to frame the modeling problem at hand in order to gain a systems-level understanding of the interaction between the hydrodynamic forces and adhesive forces at play in the perfused microenvironment provided by the multiwell bioreactor.

Chapter 2

System Model

Introduction

In the reactor system, cells are pipetted in solution above the tissue engineering scaffold. The system starts and media flows in the downward direction in order to pull the cells down into the scaffold channels in order to form adhesive contacts with the collagen coated scaffold and adjacent cells. As a result, each channel fills with a number of individual hepatocytes that through time will adhere to one another and form a tissue. However, the distribution of cells is heterogeneous. When 800,000 cells are seeded into an 800-channel scaffold, the expectated average distribution is 1000 cells per channel. However, the number of cells in each channel may vary yielding a variety of hepatocyte distributions that may influence the observed flow patterns within each channel. Two representative channel packing conditions will be considered in this chapter. An additional dynamical model proposed by Hammer et al will also be considered. The first packing condition is the ideal condition in which a planar array of cells perfectly packs the channel in a square array. This condition will be heretofore referred to as "the packed channel." Deviating from the idealized

situation, another candidate packing condition is one in which the channel is not packed in a planar array but rather partially filled. Given different paths over which the fluid may traverse, the fluid velocities will vary; in such cases, one fluid velocity may dominate yielding very different transport conditions than the packed channel condition. The channel that is not completely packed, heretofore referred to as "the partial channel", merits further analysis as well as it is representative of another potential experimental situation that yields different force and stress values. The model proposed by Hammer et al concerns receptor-mediated adhesion of cells in a shear field of viscous fluid to surfaces coated with ligand molecules complementary to the receptors in the cell membrane.

2.1 Packed Channel Model

In the introduction, three models were proposed and described. In this section, the "packed channel" model will be considered.

2.1.1 Model Description

The "packed channel" is characterized by a full planar square array of cells that completely fills the channel. The hepatocytes are all modeled as hard spheres with radii of 10 μm. Perfused flow is upward through the array of cells with a velocity v_0. A schematic is shown in Figure 2.1.

2.1.2 Hydrodynamic Force Analysis

In the previously described model, flow in the system was evenly distributed as a result of even and distributed cell seeding across all channels. However, in cases when large areas of the channel are not covered by cells the flow moves through the path of least resistance and will be discussed

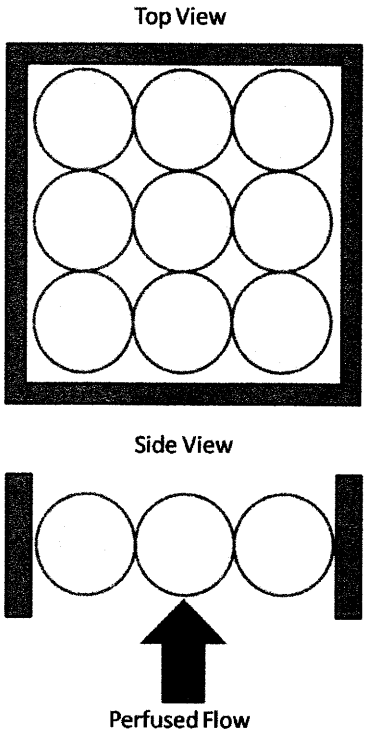

Figure 2.1: Packed Channel Model.

in the "partial channel" model.

In order to examine this model, the Navier-Stokes equations can help guide the analysis of the problem. The Navier-Stokes equation in spherical form is given in Equation 2.1.

$$\frac{\partial \rho}{\partial t} + \frac{1}{r^2}\frac{\partial(\rho r^2 v_r)}{\partial r} + \frac{1}{r\sin\theta}\frac{\partial(\rho v_\theta \sin\theta)}{\partial \theta} + \frac{1}{r\sin\theta}\frac{\partial(\rho v_\phi)}{\partial \phi} = 0 \tag{2.1}$$

where ρ is the fluid density, v_r is the radial velocity, and v_ϕ v_θ are the angular velocities.

$$\rho\left(\frac{\partial v}{\partial t} + v \cdot \nabla v\right) = -\nabla p + \mu \nabla^2 v + f \tag{2.2}$$

Analysis of a complex arrangement such as that presented by a planar array of cells would computationally intensive. Instead, an approach that is more amenable to thorough analysis would be to analyze a simpler system involving just one cell. A diagram of the simplified model is shown in Figure 2.2. The simplification presented here will be analyzed via computational means in order to justify the simplifying assumptions.

A few simplifications and assumptions of the physical system governed by the Navier Stokes equations presented in Equations 2.1 and 2.2 are in order. The first assumption is that the system is at steady state. In order to justify this assumption, the analysis of this system can be restricted to begin at the point at which the flow is fully developed. Additionally, while the pump integrated into the bioreactor generates pulses of a certain frequency, the integrated inline filter and capacitor work in concert to effectively dampen the pulses generated by the micropump [2]. Evidence of this

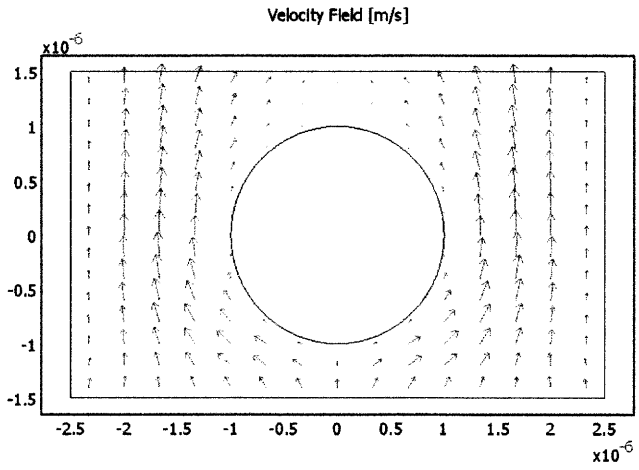

Figure 2.2: Single Sphere Simplification.

is shown in Figure 2.3. Additionally, given the low fluid velocities, the Reynolds number is much less than one.

Furthermore, upon consideration of the Navier-Stokes equations, the system is symmetric in the ϕ direction. In turn, $u_\phi \to 0$ and $\frac{\partial}{\partial \phi} \to 0$. Combining the continuity equations and Navier Stokes equations results in the following equation.

$$\frac{\partial u_r}{\partial r} + \frac{2u_r}{r} + \frac{1}{r}\frac{\partial u_\theta}{\partial \theta} + \frac{u_\theta \cot\theta}{r} = 0$$

$$0 = -\frac{1}{r}\frac{\partial P}{\partial \theta} + \mu\left(\frac{\partial^2 u_\theta}{\partial r^2} + \frac{2}{r}\frac{\partial u_\theta}{\partial r} - \frac{u_\theta}{r^2 \sin^2\theta} + \frac{1}{r^2}\frac{\partial^2 u_\theta}{\partial \theta^2} + \frac{\cot\theta}{r^2}\frac{\partial u_\theta}{\partial \theta} + \frac{2}{r^2}\frac{\partial u_r}{\partial \theta}\right)$$

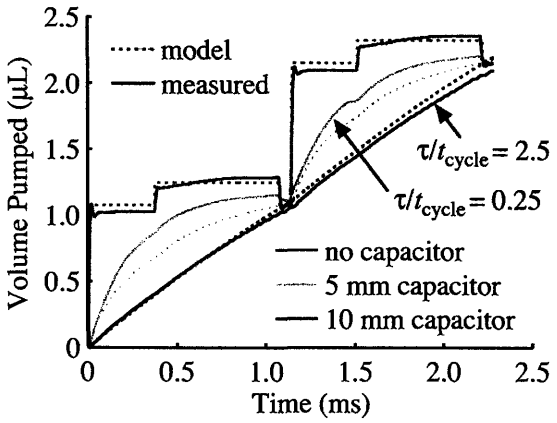

Figure 2.3: Evidence showing pulsatility reduction [2].

By applying the no-slip boundary conditions at the surface and assuming $u_r \to u_0 \cos\theta$ and $u_\theta \to -u_0 \sin\theta$ as $r \to \infty$. The solutions for u_r, u_θ, and P are given by equations 2.3, 2.4, 2.5.

$$u_r = u_0 \cos\theta \left[1 - \frac{3}{2}\frac{a}{r} + \frac{1}{2}\frac{a^3}{r^3}\right] \tag{2.3}$$

$$u_\theta = -u_0 \sin\theta \left[1 - \frac{3}{4}\frac{a}{r} - \frac{1}{4}\frac{a^3}{r^3}\right] \tag{2.4}$$

$$P - P_0 = \mu u_0 \cos\theta \left(\frac{-3a}{2r^2}\right) \tag{2.5}$$

Integrating this viscous stress $-\mu\left(\frac{\partial u_\theta}{\partial r}\right)$ and pressure over the area of the sphere, the resulting total force on the sphere is given by the solution for Stokes Drag over a sphere shown in equation 2.6.

$$F_D = 6\pi\mu R u_0 \tag{2.6}$$

This result equation provides a means to analyze the hydrodynamic forces imposed by a free stream velocity of u_0. The following section will provide a means for analyzing the adhesive forces created by the integrins and cadherins involved in mediating the adhesion between adjacent cells and extracellular matrix.

2.1.3 Adhesive Force Analysis

Integrins and cadherins on the surface of the hepatocytes generate a certain adhesive force in order to link cells to matrix or cells to one another. In order to gain some insight about the problem, the nature of the adhesive molecules will be described as follows. The integrins and cadherins are evenly distributed over the entire surface area of the cell. The integrins and cadherins do not cluster. Finally, only a fraction of the CAMs on the surface of the cell are involved in cell adhesion.

With these assumptions, an expression for the adhesive force generated by the integrins can be derived. This is shown in Equation 2.7.

$$F_i = f_i \cdot N_I \cdot y \tag{2.7}$$

where f_i is the force generated by an individual integrin, N_I is the number of integrins per cell, and y is the percent of the cell surface area involved in integrin mediated adhesion.

Similarly, an expression for the adhesive force generated by the caherins can be derived. This is shown in Equation 2.8.

$$F_c = f_c \cdot N_C \cdot w \tag{2.8}$$

where f_c is the force generated by an individual cadherin, N_C is the number of integrins per cell, and w is the percent of the cell surface area involved in cadherin mediated adhesion.

2.1.4 Interaction between Hydrodynamic Forces and Adhesive Forces

Combining the adhesive force model with the hydrodynamic force model and considering the goal of the device to build tissues from single cells, the adhesive force should be greater than the hydrodynamic forces generated by a given free stream fluid velocity. This relationship is given by the Equation 2.9 or 2.10 depending on the cell adhesion molecules involved in adhesion.

$$F_D < F_i \tag{2.9}$$

$$F_D < F_c \tag{2.10}$$

Using reported values for the model parameters, ranges for acceptable flow rates can be selected in order to operate the bioreactor at optimal conditions.

2.2 Partial Channel Model

In the introduction, three models were proposed and described. In this section, the "partial channel" model will be considered.

2.2.1 Model Description

The "partial channel" is characterized by a random arrangement of cells resulting in a channel that it partially filled. Again, the hepatocytes are all modeled as hard spheres with radii of 10 μm. Perfused flow is upward through the array of cells with a velocity v_0. A schematic is shown in Figure 2.4.

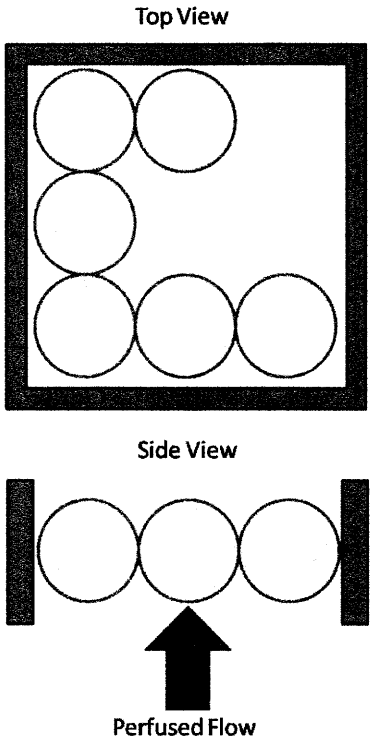

Figure 2.4: Partial Channel Model.

2.2.2 Hydrodynamic Force Analysis

In the "packed channel" model, the flow was evenly distributed across the entire area as a result of two effects. The first effect was due to the inline filter serving as a resistive element to distribute flow over the entire scaffold area. The second was due to the equally distributed placement of the cells in the channel. In the case of the "partial channel," however, the unequal distribution of cells in the channel results in different mass transport models. A commonly observed distribution of cells observed in experimental situations is one in which the cells form a donut-like shape in which cells adhere to the sides of the channel wall and form a conduit for fluid flow at the center. Creating a model analog to this situation, the physical situation can be described as pipe flow. The conduit cross-section can be modeled with different shapes and sizes, but basic insights can be gained by modeling the channel as forming a cylindrical conduit shown by Figure 2.5.

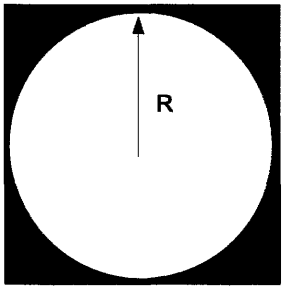

Figure 2.5: Partial Channel Model. The dark areas represent tissue and the white area represents void space.

Assuming that transport of the media will be through the path of least resistance, the Navier Stokes equations can again be employed to analyze the underlying physics of the fluid transport. The Navier-Stokes equation in cylindrical form is given in Equation 2.11.

$$\frac{1}{r}\frac{\partial}{\partial r}(ru_r) + \frac{1}{r}\frac{\partial u_\theta}{\partial \theta} + \frac{\partial u_z}{\partial z} = 0 \tag{2.11}$$

$$\rho\left(\frac{\partial v}{\partial t} + v \cdot \nabla v\right) = -\nabla p + \mu\nabla^2 v + f \tag{2.12}$$

Similar to the "packed channel" model, a few simplifications and assumptions of the physical system governed by the Navier Stokes equations presented in Equation 2.11 and 2.12 are in order. The first assumption is that the system is at steady state. In order to justify this assumption, the analysis of this system can be restricted to begin at the point at which the flow is fully developed. Again, the pulses of the pump are considered insignificant because they are dampened by the presence of the inline filter and capacitor. The medium, again, is considered incompressible.

Furthermore, upon consideration of the Navier-Stokes equations, the system is symmetric in the θ direction. In turn, $u_\theta \rightarrow 0$ and $\frac{\partial}{\partial \theta} \rightarrow 0$. Combining the continuity equations and Navier Stokes equations results in the following equation.

$$0 = -\frac{dP}{dz} + \mu\frac{d^2 v_z}{dr^2}$$

By applying the no-slip boundary conditions at the perimeter of the conduit, assuming that the system is symmetric ($\frac{\partial v_z}{\partial r} = 0$), and assuming that $-\frac{dP}{dz}$ is constant, expressions for the channel velocity are obtained. The solutions for $v_z(r)$is given by equation 2.13.

$$v_z(r) = 2\overline{v}\left(1 - \left[\frac{r}{R}\right]^2\right), \tag{2.13}$$

where $\overline{v}$ is the flow-averaged mean velocity.

$$\overline{v} = \frac{\int_0^R v_z(r) 2\pi r dr}{\int_0^R 2\pi r dr}$$

With an expression for the fluid velocity in the channel, the shear stress at the fluid-tissue interface can be determined. The expression is given by Equation 2.14.

$$\tau_{rz} = -\mu \frac{dv_z}{dr} = -\frac{4\mu\overline{v}}{R} \tag{2.14}$$

Integrating this viscous stress over the surface of the area formed by the conduit, the resulting total force is given by Equation 2.15.

$$F_S = \int\int \tau_{rz} dA = 2\pi Rh\left(\frac{4\mu\overline{v}}{R}\right), \tag{2.15}$$

where h is the height of the cylindrical channel formed by the cells.

Recognizing, however, that the height of the channel in this case is the diameter of the cells, Equation 2.15 now becomes:

$$F_S = \int\int \tau_{rz} dA = 2\pi Rh\left(\frac{4\mu\overline{v}}{R}\right) = 2\pi R(2R_{cell})\left(\frac{4\mu\overline{v}}{R}\right) = 16\pi R_{\text{cell}}\mu\overline{v} \tag{2.16}$$

Furthermore, recognizing that the average velocity is given by the volumetric flow rate over conduit area, the shear force becomes:

$$F_S = \frac{16R_{\text{cell}}\mu q}{R^2}$$

This result equation provides a means to analyze the hydrodynamic forces imposed by a free stream velocity of u_0. The following section will provide a means for analyzing the adhesive forces created by the integrins and cadherins involved in mediating the adhesion between adjacent cells and extracellular matrix.

2.2.3 Adhesive Force Analysis

In this model, the fluid shear acts to disrupt the adhesive links between the cells at the fluid tissue interface and the cells and matrix proteins that they are near. The assumptions and approximation made in the case of the "packed channel" model are again valid here. In summary, the cell adhesion molecules do not cluster. They are evenly distributed over the entire surface of the cell. Finally, only a fraction of the cell adhesion molecules are employed in adhesion.

Combining the model geometry with the assumptions concerning the behavior of the integrins and cadherins, an expression for the adhesive force generated can be derived and is shown in Equation 2.17.

$$F_{s,i} = f_i \cdot i_A \cdot A \cdot y \tag{2.17}$$

where f_i is the force generated by an individual integrin, i_A is the number of integrins per unit area, A is the surface area of the cell-fluid interface, and y is the percent of the cell surface area involved in integrin mediated adhesion.

Similarly, an expression for the adhesive force generated by the caherins can be derived. This is

shown in Equation 2.18.

$$F_{c,i} = f_c \cdot c_A \cdot A \cdot w \tag{2.18}$$

where f_c is the force generated by an individual cadherin, c_A is the number of integrins per unit area, A is the surface area of the cell-fluid interface, and w is the percent of the cell surface area involved in integrin mediated adhesion.

2.2.4 Interaction between Hydrodynamic Forces and Adhesive Forces

As with the "packed channel", the adhesive force should be greater than the hydrodynamic forces generated by a given free stream fluid velocity. This relationship is given by the Equation 2.19 or 2.20 depending on the cell adhesion molecules involved in adhesion.

$$F_S < F_{s,i} \tag{2.19}$$

$$F_S < F_{c,i} \tag{2.20}$$

Using reported values for the model parameters, ranges for acceptable flow rates can be selected in order to operate the bioreactor at optimal conditions.

2.3 Hammer Model

A wide body of literature exists that describes the behavior of cells under flow inspired by adhesion of blood-borne cells to the vascular surface in the inflammatory system and cancer cell metastasis. Hammer et al have recommended a model to describe receptor-mediated adhesion to a surface

depicted by Figure 2.6 [3].

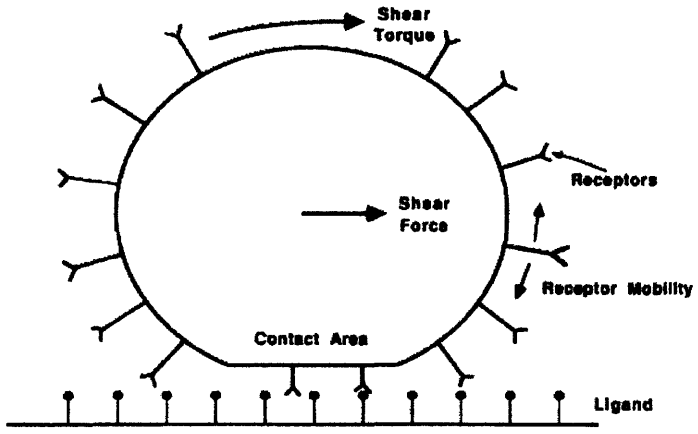

Figure 2.6: Physical Description of Dynamical Model proposed by Hammer et al [3].

The authors make several assumptions which ultimately lead to an expression for the total force of the cell under flow. At close approach, pressure builds up between the cell and the surface and the portion of the cell closest to the surface flattens. This flattened area is the contact area over which adhesion occurs. The contact area is also assumed to be constant with time. The authors also assume that they can approximate the normal stress distribution such that the bonds are equally stressed in the contact area.

In this model, the adherent cell is assumed to be in mechanical equilibrium and has no net force or torque working on it. The shear force is balanced by the bond force, and the torque imposed by the fluid flow is counteracted by the torque from the bonding force. The resulting expression for the total force is given by Equation 2.21.

$$F_t = 6\pi\mu R_c^2 SR \cdot \sqrt{\left(1+\frac{S}{R_c}\right)F^{s^2}\left(1+\frac{9\pi^2 R_c^2}{16a^2}\right)+\left(1+\frac{S}{R_c}\right)F^2\tau^s\frac{3\pi^2 R_c^2}{4a^2}F^s\tau^s\left(1+\frac{S}{R_c}\right)+\frac{\pi^2 R_c^2}{32a^2}\tau^{s^2}} \tag{2.21}$$

where S is separation distance, R_c is the cell radius, a is the radius of the contact area, SR =shear rate, μ is the media viscosity, and F^s and τ^s are functions of dimensionless separation distance only.

Chapter 3

Results

Introduction

Using the models and equations proposed in the prior chapter, a variety of flow conditions can be analyzed as a means to interpret the effects on hydrodynamic forces on cell adhesion. In summary, two models were proposed describing a completely packed channel and a partially packed channel, and a third was taken from the literature. These models led to mathematical analyses that took advantage of either the solution for Stoke's Drag around a sphere or channel flow. Comparing the hydrodynamic forces to the forces involved in adhesion, one can determine values for the flow rates that will not interfere with the inherent adhesive forces employed by the cadherins and integrins.

3.1 Packed Channel Model

3.1.1 Stokes Drag Simplification

One approximation made in the "packed channel" model is that instead of modeling the entire planar array that one could analyze just one sphere. In order to justify this assumption, presented below are the results of two different analyses, one using finite element modeling and the other using first principles. Using a commercially available finite element package, the following situation was modeled. A square planar (2x2) array of four cells with radii 10 μm were subject to perfused flow shown in Figure 3.1. An array of only 4 spheres was chosen because the inlet boundary condition is set with a fluid velocity and not a volumetric flow rate in which the area over which flow occurs is important. As a result, additional spheres would only have increased the time to reach a solution as additional spheres generate additional nodes at which the partial differential equations must be solved.

In order to achieve rough approximations of the velocity and shear stress, the incompressible Navier-Stokes equation is used in the form described by Equation 2.2.

The Navier-Stokes problem has the following boundary conditions:

- A prescribed inlet velocity, v_0, below the array
- An outlet pressure of zero, $p_{out} = 0$, above the cell
- No slip boundary conditions everywhere else

The values for the variables used in the model are summarized below in 3.1.

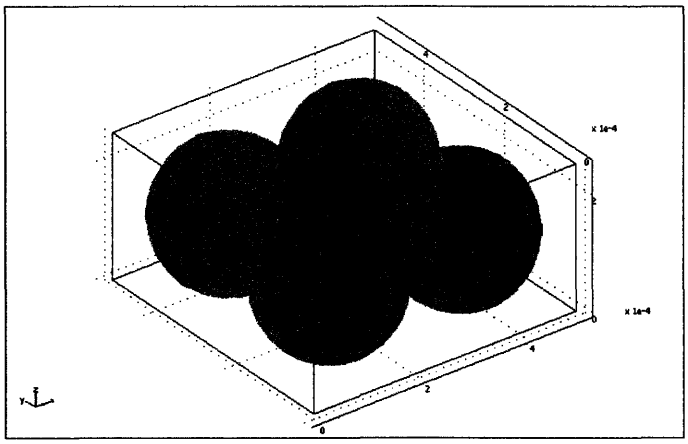

Figure 3.1: 3D Model Geometry

Table 3.1: Variable Values as Used in Stokes Drag Model

Variable	Value
Free Stream Velocity [m/s]	v_0
Media Viscosity [Pa·s]	$8.4 \cdot 10^{-4}$
Hepatocyte Radius [m]	10^{-6}

For the purpose of visualizing the shear stress solely on the surface of the cell, an imaginary variable, τ_{surf} is employed as the sum of the shear stresses as solved for by the Navier Stokes equations.

Despite additional computational demands, a direct solver still can compute the solution in a reasonable amount of time. This three-dimensional model has 1342 elements. Solving for the solution to only one equation system results in 19733 degrees of freedom. UMFPACK, a linear solver, is the

preferred solver because it is a highly efficient solver in situations involving unsymmetric equation systems [14].

The solution achieved is as expected. On a Pentium M 1.6 GHz computer with 512 MB of RAM, the static solver took roughly 70 seconds to solve.

For the presented solution, the inlet velocity, v_0 is 100μ/s.

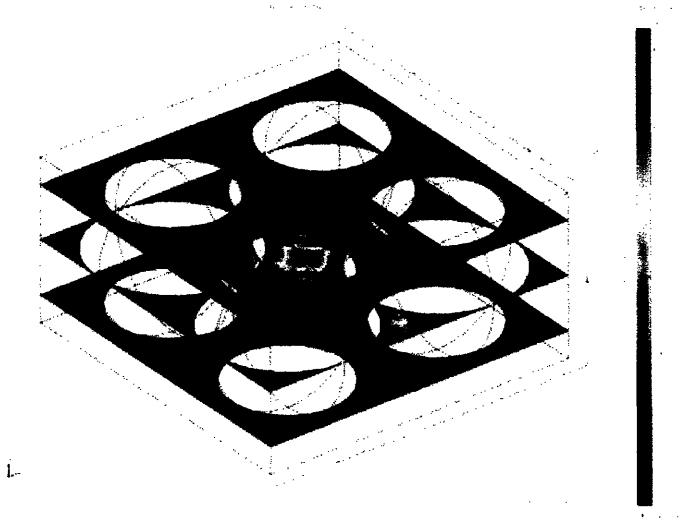

Figure 3.2: Velocity Field between Cells Modeled as Hard Spheres

Figures 3.2 and 3.3 demonstrate the ability to evaluate the velocity field and shear stress distribution. Figure 3.2 shows that the highest velocities are observed in the central regions between the cells, and Figure 3.3 shows that the shear stress is evenly distributed over the surface in the case

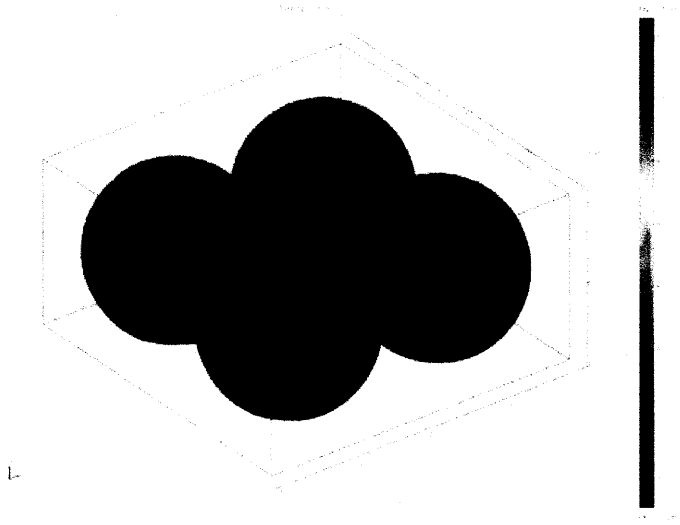

Figure 3.3: Surface Shear Stress on Cells Modeled as Hard Spheres

of hard spheres.

Comparing the stress values reported by the finite element solution and the solution achieved by first principles justifies the assumption made to simplify the planar array to just one sphere where the Stokes drag solution could be used.

3.1.2 Sensitivity Analysis

Equation 2.6 gives an expression for the Stoke's Drag on a sphere. In this model, the sphere is a cell in the array of perfused cells. Looking at the equation, the observed force has a first order relationship with all variables in the expression. Therefore, the observed force is equally responsive

to all variables equally.

3.1.3 Force Comparisons

The relationships introduced by Equations 2.9 and 2.10 yield the summarized results.

The values for the variables used in the adhesive model are summarized in Table 3.2:

Table 3.2: Variable Values as Used in Adhesive Model

Variable	Value
Total Number of Integrins per Cell	10^5
Force per Integrin	$1 - 10$ pN

Using the proposed model, the appropriate variable to vary is y since this value is not widely reported or easily measurable. Figure 3.4 shows the predicted upper-bound and lower-bound values for adhesive forces generated by a single hepatocyte. The blue line predicts the adhesive behavior in the case where the integrin force is 10 pN, and the red line predicts the adhesive behavior when the integrin force is 1 pN. The entire region between these two lines are potential force estimates as the probable case is that the bond forces are not homogeneous at either the upper or lower bound.

Now that ranges for the adhesive forces have been determined, it is also important to compare these adhesive forces to those associated with Stokes drag. The important transition to notice is the point where the hydrodynamic forces are greater than the adhesive force. In order to build tissue constructs, one would want to operate the multiwell bioreactor at flowrates that do not inhibit

Figure 3.4: Adhesive Force Generated by Cell Adhesion Molecules

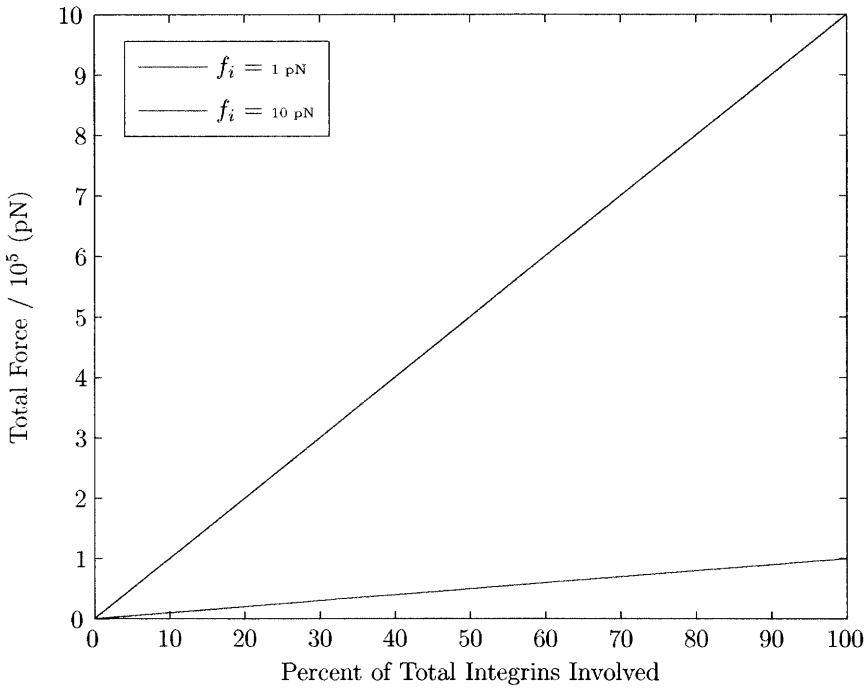

integrin or cadherin binding.

Evaluating the results of 2.6,2.7, and 2.8 over a range of characteristic values, one can compare the forces that can be generated by the perfused flow and those that can be generated by integrin and cadherin bond formation. In Table 3.3, the ranges presented for the cadherin and integrin binding forces range from the case where no cell adhesion molecules are involved in binding to where either all cadherins or all integrins are engaged. Similarly, for the range of force values presented for the Stokes Drag solution ($6\pi\mu Rv_\infty$) includes ranges of values for hepatocyte radii above and below the reported mean of 10μm and velocities ranging from $0 - 200\mu$m/s which represents the typical flow velocities used in the culture system.

Table 3.3: A comparison of the forces generated by Stokes Drag, Integrins, and Cadherins in "Packed Channel Model"

Force Generated By:	Minimum [pN]	Maximum [pN]
Stokes Drag	0	35.15
Integrins	0	10^6
Cadherins	0	10^6

As Table 3.3 demonstrates, even in cases where a small fraction of the cell adhesion molecules engage, according to the proposed model, the adhesive force presented by the integrins and cadherins is greater than the drag force that results from the fluid flow.

In order to determine the flowrates necessary to mechanically disrupt the integrin or cadherin mediated bonds, by setting the hydrodynamic force equal to the adhesive force from integrins or cadherins and solving for u_∞, the following expressions emerge.

$$u_\infty = \frac{N_i f_i y}{6\pi R\mu}$$

or

$$u_\infty = \frac{N_c f_c w}{6\pi R\mu}$$

Assuming that only ten percent of either the cadherins or the integrins are engaged, the velocity necessary to physically disrupt the bonds is 0.6316 m/s which is extremely high. Even if all cadherins or integrins are engaged, the velocity only reduces ten-fold.

Using the physical framework set forth by the "packed channel" model, the force generated by the perfused flow does not seem to be sufficient to pull the cells away from the extracellular matrix or from neighboring cells. These results provide disparate values for the hydrodynamic force compared to the adhesive biological forces. Experimental observations at these flow rates suggest that the hydrodynamic forces do inhibit the formation of tissue. This suggests that the model proposed by using a Stoke's Drag analysis underestimates the value of the hydrodynamic forces.

3.2 Partial Channel Model

3.2.1 Channel Flow Simplification

A key aspect of the partial channel model involved making the assumption that fluid travels through the path of least resistance.

An equivalent fluidic circuit can be built to describe the physics of the fluid flow. Realizing that this system can be modeled as a current divider where the resistive element is the microporous filter and the cells above it or the microporous filter alone. The circuit is shown below in Figure 3.5.

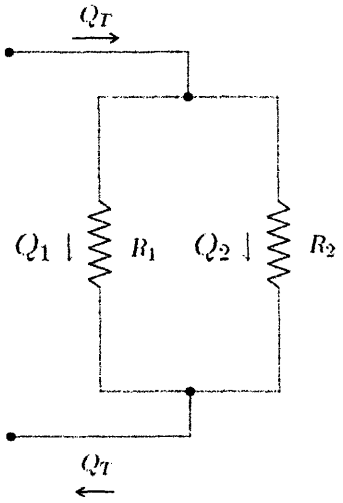

Figure 3.5: Simplified Fluidic Circuit derived from Physical Model

Using the current divider analogy, the current or mass flow through the channels can be described by the following equations:

$$Q_1 = Q_T \frac{R_2}{R_1 + R_2}$$

$$Q_2 = Q_T \frac{R_1}{R_1 + R_2}$$

As demonstrated by these equations if the resistances are equal, the fluid flow is roughly the same

through both the tissue and the conduit formed by the tissue. However, if $R_1 >> R_2$, the flow through branch 2 will be much greater than the flow through branch 1. Given the results of this analysis, treating the fluid flow in this case as channel flow seems like an appropriate approximation.

In order to achieve rough approximations of the velocity and shear stress, the incompressible Navier-Stokes equation is used in the form described by Equations 2.11 and 2.12.

The Navier-Stokes problem has the following boundary conditions:

- A prescribed volumetric flow, q_0, at the inlet
- No slip boundary conditions at $r = R$

The values for the variables used in the model are summarized below in 3.4.

Table 3.4: Variable Values as Used in Packed Channel Model

Variable	Value
Volumetric Flowrate [m^3/s]	q_0
Media Viscosity [Pa·s]	$8.4 \cdot 10^{-4}$
Hepatocyte Radius [m]	10^{-6}

Another key assumption made is that for such low flowrates, there are no flow-induced deformations meaning that the cells can be modeled as hard spheres once again.

3.2.2 Sensitivity Analysis

Equation 2.15 gives an expression for the hydrodynamic force exerted on the hepatocytes at the fluid tissue interface. Again, in this model, similar to the "packed channel" model, all variables

have an equal influence on the force via a first order relationship.

3.2.3 Force Comparisons

The relationships introduced by Equations 2.17 and 2.18 yield the summarized results.

The values for the variables used in the adhesive model are summarized earlier in Table 3.2.

Using the proposed model, the appropriate variable to vary is y since this value is not widely reported or easily measurable. Figure 3.6 shows the predicted upper-bound and lower-bound values for adhesive forces generated by a single hepatocyte. The blue line predicts the adhesive behavior in the case where the integrin force is 10 pN, and the red line predicts the adhesive behavior when the integrin force is 1 pN. The entire region between these two lines are potential force estimates as the probable case is that the bond forces are not homogeneous at either the upper or lower bound. It is expected that in this model, given that the analysis focuses on cells at the fluid-cell interface that less than fifty percent of the integrins will actually be physically engaged in adhesive interactions.

Now that ranges for the adhesive forces have been determined, it is also important to compare these adhesive forces to those associated with fluid shear force. Identical to the rationale presented in the "packed channel" model, in order to build tissue constructs, one would want to operate the multiwell bioreactor at flowrates that do not inhibit integrin or cadherin binding.

Plotting the results of Equations 2.15, 2.17, and 2.18 over a range of characteristic values, one can

Figure 3.6: Range of Adhesive Forces Generated by Cell Adhesion Molecules

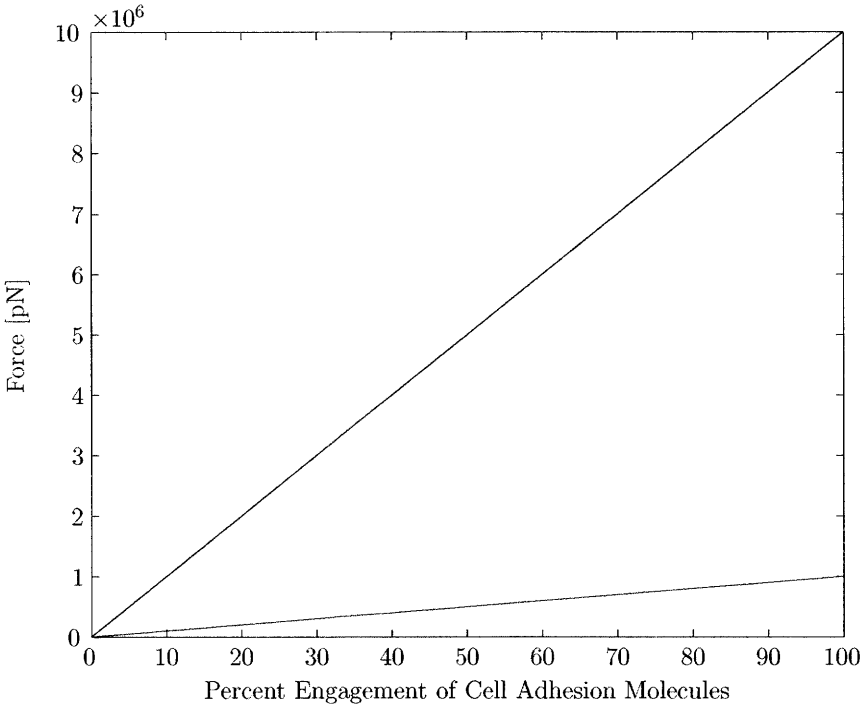

compare the forces that can be generated by the perfused flow and those that can be generated by integrin and cadherin bond formation. In Table 3.5, the ranges presented for the cadherin and integrin binding forces range from the case where no cell adhesion molecules are involved in binding to where either all cadherins or all integrins are engaged. Similarly, for the range of force values presented for the shear force solution includes ranges of values for hepatocyte radii above and below the reported mean of 10μm and velocities ranging from $0-1$ μL/channel-min which represents the typical volumetric flow rates used in the culture system.

Table 3.5: A comparison of the forces generated by Shear Stress, Integrins, and Cadherins in "Partial Channel Model" assuming $R = 100\mu$m

Force Generated By:	Minimum [pN]	Maximum [pN]
Shear Force	0	224
Integrins	0	10^7
Cadherins	0	10^7

As Table 3.5 demonstrates, even in cases where a small fraction of the cell adhesion molecules engage, according to the proposed model, the adhesive force presented by the integrins and cadherins is greater than the drag force that results from the fluid flow.

In order to determine the volumetric flow necessary to mechanically disrupt the integrin or cadherin mediated bonds, by setting the hydrodynamic force equal to the adhesive force from integrins or cadherins and solving for q, the following expressions emerge.

$$q = \frac{N_i f_i y R}{16\mu}$$

or

$$q = \frac{N_c f_c w R}{16\mu}$$

Assuming that only ten percent of either the cadherins or the integrins are engaged ($f_i = f_c = 1\text{pN}$) and a conduit with radius $R = 100\mu\text{m}$, the volumetric flow rate necessary to physically disrupt the bonds is approximately 4.5 μL/channel·minute.

Using the "partial channel" model, again, the force generated by the perfused flow does not seem to be sufficient to pull the cells away from the extracellular matrix or from neighboring cells.

These "partial channel" and "packed channel" provide a simplified analysis of the physical situation. If the cells were deforming, nonuniformities would exist in the velocity field and the forces that will tend to break the bonds may operate more in shear than in tension, however such complications are not treated here. Again, the values for the hydrodynamic forces and adhesive forces are very disparate. At high flow rates, we experimentally observe different behavior than what this model suggests. This suggests that while the "packed channel" model is mathematically correct, it cannot fully capture the physical behavior of the system.

3.3 Hammer Model

The model proposed by Hammer et al resulted in an equation for the force on a cell described by Equation 2.21. Using the the parameter values summarized by Table 3.6, we calculate the total force on the cell.

Table 3.6: Variable Values as Used in Hammer Model

Variable	Value
Hepatocyte Radius (R_c) [m]	$10 \cdot 10^{-6}$
Shear Stress ($SR \cdot \mu$) ($\dot{q} = 1\mu$L/channel·min)	0.0043
Contact Area Radius (a)	$1 \cdot 10^{-6}$
F^s[15]	1.7
τ^s[15]	0.94
Separation Distance (S) [m]	$0.99 \cdot 10^{-10}$ [16]

The adhesive force of the CAMs is given by:

$$F_a = \frac{\pi a^2}{4\pi R_c^2} \cdot N_c \cdot f_c \tag{3.1}$$

where F_a is the adhesive force, a is the contact area radius, R_c is the cell radius, N_c is the total number of CAMs per cell, and f_c is the strength of an individual bond.

Using these values, the calculated value for the force due to flow is approximately 400 picoNewtons. Comparing these forces to the inherent biological forces over the projected contact area, the calculated biological force is approximately 250 picoNewtons assuming that the CAMs are evenly distributed over the surface of the cell and have a force of 1 pN each. For this volumetric flow rate, the hydrodynamic forces are greater than the biological forces suggesting that at this flow rate the hydrodynamic forces inhibit bond formation. These results seem coincide with experimental

observations. However, at the same time, the physical model built by Hammer et al does not fully capture the complexity within a scaffold channel because the Hammer model treats one cell under flow where our system has multiple cells under flow with several regions of adhesive contacts. Nonetheless, as a first order analysis, the Hammer model has provided results that agree best with experimental observations.

3.4 An Alternative Approach to Understanding Adhesion

The three models proposed in this thesis involved simplifying the kinetics of cell adhesion mediated by cadherins and integrins to a model situation where permanent bonds with a certain bond strength formed with no dependence upon ligand or receptor concentration or bond association and disassociation rates. The "packed channel" and "partial channel" models also provided disparate values between the hydrodynamic and adhesive forces generated by the CAMs. While these models have provided some insight into how to model the system appropriately, models that provide better agreement with experimental results are much more powerful. It is therefore important to consider modifications to the model that can better predict system behavior.

From a chemical kinetics perspective:

$$R + L \rightleftharpoons R \cdot L$$

where R is the receptor concentration, L is the ligand concentration, and $R \cdot L$ is the ligand-receptor complex concentration. The reaction has a association rate k_f and a dissociation rate of k_r.

While this chemical equilibrium equation does not explicitly involve hydrodynamic forces in order

to describe the behavior, incorporating the Bell Model for cell adhesion can help to potentially explain the observed behavior[17]. The Bell Model is described by Equation 3.2.

$$k_r = k_{r_0} \exp\left(\frac{\gamma f}{k_B T}\right) \tag{3.2}$$

where k_{r_0} is the unstressed disassociation rate, γ is a factor with units of length that approximately corresponds to the distance separating the bonded pair at equilibrium, f is the external force applied on a given bond, and $k_B T$ is the energy.

To understand the ramifications of the Bell Model on the model presented here, one can plug in the values for the forces generated in the three models 3.2 for f. The temporal behavior of the concentration of bound complexes can be described by Equation 3.3.

$$\frac{dC_B}{dt} = k_f(C_R - C_L) - k_r C_B = k_f(C_R - C_L) - k_{r_0}\left(\frac{\gamma f}{k_B T}\right) \tag{3.3}$$

where k_f is the bond association rate, k_r is the bond disassociation rate, C_R is the receptor concentration, C_L is the ligand concentration, and C_B is the concentration of bound receptor-ligand complexes.

By solving the differential equation for C_B one can determine the number of bonds present at any time.

As demonstrated by the Bell Model, increased force increases the dissociation rate for receptor-ligand complexes in cellular systems. Combining this analysis with what what has been developed by the proposed physical models earlier in this chapter to experiments that have shown loading

rates to influence cell adhesion, one can better understand the various ways that forces influence cell adhesion in this system.

3.5 Conclusion

Three models were proposed as a means to evaluate the effects of hydrodynamic forces on cell adhesion in a perfused bioreactor. Two models, the "packed channel" and "partial channel" models yielded with disparate values between the hydrodynamic forces and the adhesive forces. However, the model proposed by Hammer et al was much more successful at providing values for the hydrodynamic force and biological force of the same order of magnitude such that competitive interactions could be observed.

Chapter 4

Conclusions and Future Directions

4.1 Summary

The overall aim of this thesis research was to explore one of the many signals that influence successful formation of tissue from single cells in a perfused tissue bioreactor. Figure 4.1 summarizes the known positive and negative cues known to influence tissue engineering applications such as the one motivating this thesis.

It was hypothesized that the hydrodynamic forces and shear stresses generated by the presence of the perfused flow may inhibit the formation of bonds or break the bonds mediated by the presence of cell adhesion molecules such as integrins or cadherins. To this end, two models were developed in order to describe the mechanical behavior of the system by using an analysis that employed Stokes drag on a sphere or flow through a pipe. A third model from the literature was also employed. Comparing these forces to the forces generated by integrin or cadherin bonds allows one to determine if the forces generated by flow inhibit bond formation or disrupt the mechanical integrity of

existing bonds.

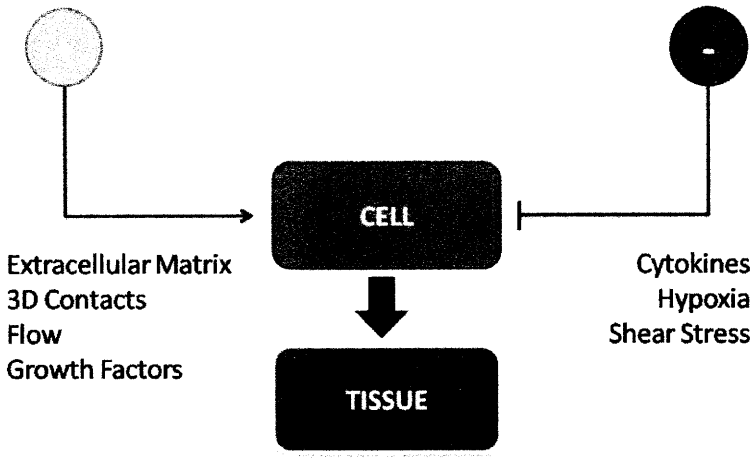

Figure 4.1: This flowchart outlines the positive and negative signals involved with this application of tissue engineering.

The result of the analyses of both the "packed channel" and "partial channel" models demonstrated that the forces generated by flow do not have an adverse effect on the mechanical integrity of the bonds. However, these results did not appear to agree with observed experimental behavior where reactors with lower flow rates seem to have better retention and formation of tissue constructs. The Hammer model, however, did provide values for the hydrodynamic forces and adhesive forces of the same order of magnitude suggesting that at the flowrates at which the system operates the hydrodynamic forces may break the bonds formed by the CAMs.

In order to better combine experimental observations with model predictions, an alternative model was proposed that incorporated kinetic analyses that better modeled the behavior of receptor-ligand dynamics. This analysis called upon the Bell Model which suggests that the dissociation rate of receptor-ligand complexes is positively correlated with the external force. Combining this model with the physical model may lead to better prediction of the behavior of cells under the presence of different flow rates.

4.2 Future Recommendations

4.2.1 Computational Modeling

While hydrodynamic forces and shear stresses locally felt by the cell are difficult to measure, future studies that aim to understand the role that hydrodynamic forces play on cell adhesion in perfused bioreactors may involve relaxing many of the boundary conditions and eliminating simplifications that may under or overestimate the forces generated by the integrin and cadherin-mediated bonds. For example, by allowing the cells to become deformable spheres, one could better calculate the actual contact area between neighboring cells or cells and matrix. In doing so, it would be much easier to estimate the actual hydrodynamic and adhesive forces. Computational modeling may also be harnessed to test a variety of hypothetical cell arrangements. In this thesis, two models were presented: a "packed channel" and a "partial channel" model. These models were further simplified to physical analogs of flow through a pipe or Stokes drag around a sphere. Computational modeling may better facilitate simulations of non-idealized cell arrangements and stochastic processes.

4.2.2 Physical Modeling

As mentioned earlier, the Hammer model provided the best agreement between model predictions and experimental observations. However, as shown by Figure 2.6, only one contact area is considered. In reality, any given cell in the scaffold channel may engage in several adhesive contacts with the walls of the channel coated with extracellular matrix protein or adjacent cells. Therefore, the next step in modeling this system would be to consider a cell with several adhesive contacts subject to perfused flow. Intuition may suggest that the adhesive forces in this case will be greater in this case, but as demonstrated by Equation 3.1, the adhesive force depends on the contact area radius, and in the case of more contacts, the overall contact area may remain constant or even be reduced.

4.2.3 Experimental Validation

Inspired by experimental observations, the central question of this thesis was developed. In order to better isolate the pathways through which hydrodynamic forces act in tissue engineering, a set of well defined experiments are in order to evaluate the effects of flow on cell adhesion and functional output. Since a model is only as good as the experimental conditions it can predict, complementing model predictions with experimental observations is an essential activity in order affirm model validity and elucidate the pathways through which the mechanical forces and stresses transmit a signal. While for a given flow rate the cells may adhere, adhesion is only one criterion that defines success in terms of this tissue engineering application.

Since the goal with this application is to build *in vitro* models of the liver it is important to functionally characterize the behavior of the cells in the system. A productive experiment would be

to iterate over a range of flow rates and characterize the behavior of the cells via RT-PCR and other functional assays such as metabolism or biological product formation in order to observe any flow-dependent trends.

Additionally, this system highlights an engineering challenge that would make for a very productive study. From one perspective as highlighted in the introduction, increasing the flowrate has the positive result of helping to enhance the oxygen transport in the system. At the same time, this thesis has shown using the Hammer model that at certain flowrates the bonds may be broken by the hydrodynamic forces. A set of experiments that could explore these effects by measuring the oxygen concentration in the system while also measuring the number of cells in the scaffold at the beginning and end of the experiment would help to optimize the operational parameters for the device.

In terms of the adhesion studies in this study, a valuable experiment may be to use a parallel flow chamber and characterize the adhesive properties of the cells subject to a variety of flow rates in order to determine at which flowrates the hepatocytes begin to detach in order to correlate these data back to the proposed models in order to either confirm or deny the approximations and model assumptions made by the author.

One last experiment would be to evaluate the percent of integrin activation at various flowrates in order to determine if flow encourages the activation of integrins and in turn increases the adhesive force to resist the imposed flow.

Bibliography

[1] A. Z. S. M. P. B. D. Lodish H., Berk and J. Darnell, *Molecular Cell Biology (4th Edition).* New York, NY: W.H. Freeman and Company, 2000.

[2] S. J. O. B. T. D. Inman W, Domansky K and L. G. Griffith, "Design, modeling and fabrication of a constant flow pneumatic micropump," *J Micromechanics and Microengineering*, vol. 17, pp. 891–899, 2007.

[3] H. D and D. Lauffenburger, "A dynamical model for receptor-mediated cell adhesion to surfaces," *Biophys J.*, vol. 52, pp. 475–487, 1987.

[4] J. A. Pedersen and M. A. Swartz, "Mechanobiology in the third dimension," *Ann Biomed Eng*, vol. 33, no. 11, pp. 1469–90, 2005.

[5] R. Hoffman, "To do tissue culture in two or three dimensions? that is the question.," *Stem Cells*, vol. 11, pp. 105–111, 1993.

[6] L. Griffith and M. Swartz, "Capturing complex 3d tissue physiology in vitro.," *Nat Rev Mol Cell Biol.*, vol. 7, pp. 211–224, 2006.

[7] D. B. S. R. K. L. G. G. Mark J. Powers, Karel Domansky, "A microfabricated array bioreactor for perfused 3d liver culture.," *Biotechnology and Bioengineering*, vol. 78, pp. 257–269, 2002.

[8] R. Hynes, "Integrins: Versatility, modulation, and signaling in cell adhesion," *Cell*, vol. 69, pp. 11–25, 1992.

[9] D. E. Ingber, "The mechanochemical basis of cell and tissue regulation," *Mech Chem Biosyst*, vol. 1, no. 1, pp. 53–68, 2004.

[10] S. M. Choquet D, Felsenfeld DP, "Extracellular matrix rigidity causes strengthening of integrin-cytoskeleton linkages," *Cell*, vol. 88, pp. 39–48, 1997.

[11] Z. Sun, L. A. Martinez-Lemus, A. Trache, J. P. Trzeciakowski, G. E. Davis, U. Pohl, and G. A. Meininger, "Mechanical properties of the interaction between fibronectin and alpha5beta1-integrin on vascular smooth muscle cells studied using atomic force microscopy," *Am J Physiol Heart Circ Physiol*, vol. 289, no. 6, pp. H2526–35, 2005.

[12] W. Baumgartner, P. Hinterdorfer, W. Ness, A. Raab, D. Vestweber, H. Schindler, and D. Drenckhahn, "Cadherin interaction probed by atomic force microscopy," *Proc Natl Acad Sci U S A*, vol. 97, no. 8, pp. 4005–10, 2000.

[13] W. Baumgartner, G. J. Schutz, J. Wiegand, N. Golenhofen, and D. Drenckhahn, "Cadherin function probed by laser tweezer and single molecule fluorescence in vascular endothelial cells," *J Cell Sci*, vol. 116, no. Pt 6, pp. 1001–11, 2003.

[14] T. A. Davis and I. S. Duff, "A combined unifrontal/multifrontal method for unsymmetric sparse matrices," *ACM Trans. Math. Softw.*, vol. 25, no. 1, pp. 1–20, 1999.

[15] Q. J. Cozens-Roberts C. and D. Lauffenburger, "Receptor-mediated adhesion phenomena: Model studies with the radial-flow detachment assay," *Biophys J.*, vol. 58, pp. 107–125, 1990.

[16] C. S. Zhang, X. and V. T. Moy, "Molecular basis for the dynamic strength of the integrin $\alpha_4\beta_1$/vcam-1 interaction," *Biophys J.*, vol. 87, pp. 3470–3478, 2004.

[17] G. I. Bell, "Models for the specific adhesion of cells to cells," *Science*, vol. 200, pp. 618–627, 1978.